Exchange-coupling-induced antiferromagnetic-ferromagnetic transition in $Pr_{0.5}Ca_{0.5}MnO_3/La_{0.5}Ca_{0.5}MnO_3$ superlattices

P. Padhan and W. Prellier*
Laboratoire CRISMAT, CNRS UMR 6508, ENSICAEN, 6 Bd du Maréchal Juin, F-14050 Caen Cedex, France
(Received 22 October 2004; revised manuscript received 31 January 2005; published 24 May 2005)

Superlattices built from two antiferromagnetic (AFM), charge- and/or orbital-order compounds, $Pr_{0.5}Ca_{0.5}MnO_3$ and $La_{0.5}Ca_{0.5}MnO_3$, were studied as the thickness of $La_{0.5}Ca_{0.5}MnO_3$ (LCMO) varied. High-structural-quality thin films were obtained on $LaAlO_3$ substrates using the pulsed-laser-deposition technique. An antiferromagnetic-to-ferromagnetic transition, in addition to an enhancement of the coercivity, was observed as the LCMO-layer thickness increased. The small shift in the origin of the field-cooled hysteresis loop along the field axis indicates the presence of ferromagnetic and antiferromagnetic phases in the superlattices. We attribute these features to the AFM spin fluctuations at the $Pr_{0.5}Ca_{0.5}MnO_3/La_{0.5}Ca_{0.5}MnO_3$ interfaces resulting from the strain effects.

DOI: 10.1103/PhysRevB.71.174419 PACS number(s): 75.47.Gk, 81.15.Fg, 78.67.Pt, 75.70.−i

In multilayer structures based on transition-metal compounds several fascinating magnetic properties such as oscillatory exchange coupling,[1–3] exchange bias,[4,5] and enhanced coercivity[6] have been observed. These magnetic phenomena are the interplay of exchange coupling at the interfaces of the heterostructures composed of ferromagnetic (FM) and nonmagnetic, either metallic or insulating, materials. In these heterostructures, the interfaces are rich in magnetic and structural coordinations of the transition-metal ions[7,8] through interaction processes like direct exchange, superexchange, and double exchange. The increase in coercivity is commonly observed when ferromagnetic thin film is coupled through antiferromagnetic (AFM) thin film. Several possible mechanisms have been used to explain the increased coercivity found in FM/AFM systems such as instabilities in the antiferromagnet[9,10] and inhomogeneous magnetization reversals.[11,12] Another manifestation of exchange coupling is interfacial ferromagnetism at the interfaces of the heterostructures. Ueda *et al.*[13] studied the magnetic properties of the superlattices and found that antiferromagnetic layers of $LaCrO_3$ and $LaFeO_3$ grown on (111)-oriented $SrTiO_3$ show a ferromagnetic behavior. The authors have explained the ferromagnetic behavior due to the ferromagnetic coupling between Fe^{3+} and Cr^{3+}. Takahashi *et al.*[14] studied the transport and magnetic properties of the superlattices made up of AFM $CaMnO_3$ and paramagnetic $CaRuO_3$ grown on (001)-oriented $LaAlO_3$ (LAO) and found that they show a Curie temperature (T_C) at ~95 K and a negative magnetoresistance below T_C. The authors concluded that the ferromagnetic transition with appreciable spin canting occurs only near the interface region, due to electron transfer from the $CaRuO_3$ layer to the $CaMnO_3$ layer through the interface. Looking at these examples, it is interesting to build superlattices in order to obtain novel electronic properties. For this, many types of oxides can be used and mixed-valance manganite is one of them. Moreover, the manganite compounds exhibit many fascinating electronic properties such as colossal magnetoresistance (CMR) and charge and/or orbital ordering. The latter property of charge ordering has been seen in mixed-valence manganites in particular, when the dopant concentration is close to the commensurate value $x=0.5$ (such as $Pr_{0.5}Ca_{0.5}MnO_3$ and $La_{0.5}Ca_{0.5}MnO_3$) in the reduced-bandwidth systems.[15,16] In these systems the charge-ordering gap can be collapsed by the application of a magnetic field, an electric field, high pressure, optical radiation, and electron irradiation,[17] and this results in a metallike transport below the charge-order transition temperature.

Here, we synthesized superlattices consisting of two antiferromagnetic insulator materials, $Pr_{0.5}Ca_{0.5}MnO_3$ (PCMO) and $La_{0.5}Ca_{0.5}MnO_3$ (LCMO), on (001)-oriented $LaAlO_3$ (LAO, cubic with $a_{LAO}=3.79$ Å) to investigate new magnetic and electronic properties, and our results are reported in this paper. The effect of strain-induced spin canting on the magnetoelectronic properties of the superlattices with various LCMO-layer thicknesses is studied, keeping the PCMO layer at a fixed thickness.

The samples were grown using the multitarget pulsed-laser-deposition technique at 720 °C in an oxygen ambient of 300 mtorr.[18] The deposition rates (typically ~0.38 Å/pulse) of PCMO and LCMO were calibrated for each laser pulse of energy density ~3 J/cm^2. After the deposition the chamber was filled to 400 torr of oxygen at a constant rate, and then the samples were slowly cooled down to room temperature at the rate of 20 °C/min. The superlattice structures were synthesized by repeating 15 times the bilayer comprised of 20-unit cell (u.c.) PCMO and *n*-u.c. LCMO, with *n* taking integer values from 1 to 20. In all superlattices, the top and bottom layers were 20-u.c.-thick PCMO. The samples were characterized by magnetization (M) in addition to resistivity (ρ) and x-ray diffraction (XRD). Magnetization measurements were performed at 10 K with a magnetic field along the [100] and [001] directions of LAO.

The superlattices consisting of alternate layers of PCMO and LCMO grown on (001)-oriented LAO showed (00*l*) diffraction peaks of the constituents and substrate, indicating the growth of an epitaxial, pseudocubic phase with a *c*-axis orientation. The θ-2θ scan for three samples with different spacer-layer thicknesses is shown in Fig. 1(a). These scans were recorded around the (002) reflection of these pseudocubic perovskites. The first-order satellite peak of the sample

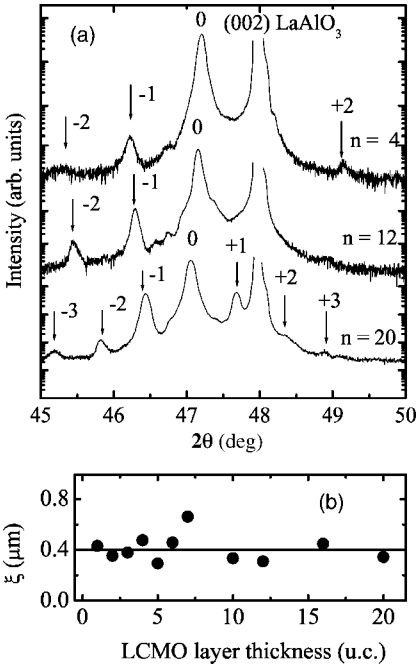

FIG. 1. (a) Reflected intensity of a $\Theta-2\Theta$ scan recorded around the (002) reflection of LAO for various superlattices. The satellite peaks of several orders (from −3 to +3) around the main peak (order 0) are indicated by arrows. n reprensents the number of LCMO layers in the PCMO/LCMO superlattice. (b) The evolution of the coherence length of the superlattices with different LCMO-layer thicknesses. The solid line is a guide to the eyes.

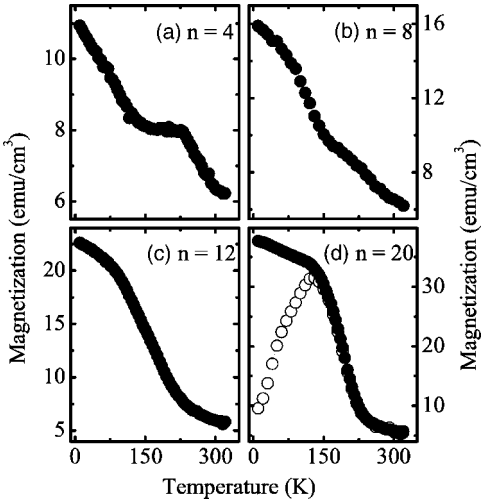

FIG. 2. Field-cooled temperature-dependent magnetization (filled circle) at 10 K at a 0.1 T out-of-plane magnetic field of various superlattices [(a): $n=4$; (b): $n=8$; and (c): $n=12$]. (d) shows zero-field-cooled temperature-dependent magnetization (open circle) and field-cooled temperature-dependent magnetization (filled circle) of the superlattice with $n=20$ at 10 K at a 0.1 T out-of-plane magnetic field.

with $n=4$ and 12 on the higher-angle-side of the (002) diffraction peak of the constituents falls on the (002) reflection of the substrate, while it is close to the (002) reflection of the substrate for the sample with $n=20$. As the LCMO-layer thickness increases, the presence of higher-order strong satellite peaks on either side of the (002) diffraction peak clearly indicates the formation of a new structure having a periodic chemical modulation of the constituents. The full width at half maximum (FWHM) of the rocking curve correlates the structural-coherence length ξ of the sample with the relation $\xi=2\pi/Q\text{FWHM}$,[20] where $Q(\approx 1/d)$ is the scattering-vector length and FWHM is in radians. The coherence length along the [001] direction of the substrate, for various samples with different LCMO-layer thicknesses, is shown in Fig. 1(b). The value of ξ is several times the total thickness of the superlattices, indicating the coherency[18] and confirming the single crystallinity of the samples seen in the XRD data.

The temperature-dependent magnetization $M(T)$ was measured in the presence of a 0.1-T magnetic field, oriented along the [001] direction of the substrate (i.e., within the plane). The field-cooled (FC) magnetization of the superlattice with $n=4$ [Fig. 2(a)] on heating from 10 K, decreases slowly up to 150 K, remains constant in the temperature range of 150 K to 230 K, and then again decreases slowly up to 320 K. This feature is qualitatively similar to that of the PCMO; i.e., the superlattice with $n=4$ displays an AFM behavior.[19] As the LCMO-layer thickness increases up to 8 u.c. [Fig. 2(b)], the FC magnetization, on heating from 10 K, decreases slowly up to 60 K, and then it drops rapidly until 170 K. Above 170 K, it increases again slowly up to 320 K. The AFM behavior observed in the sample with $n=4$ is almost suppressed in the sample with $n=8$. This AFM feature is completely suppressed for superlattices with $n\geqslant 10$, and the sample becomes FM. As an example, the temperature-dependent magnetization for $n=12$ is shown in Fig. 2(c). The magnetization decreases very slowly above 10 K up to 100 K; above this temperature the magnetization drops rapidly to 250 K and then decreases slowly up to 320 K. This temperature-dependent magnetization measured in a spin-equilibrium configuration (field-cooled) correlates with the stronger ferromagnetic interaction at the interface. Fig. 2(c) displays, for $n=20$, the magnetization measured in spin-nonequilibrium (zero-field-cooled) and spin-equilibrium configurations. This figure shows a large difference between both configurations below 100 K. This indicates the presence of an inhomogeneous nature of the spin orientations at the interfaces as well as in the bulk, due to spin canting or spin order. The increase in the LCMO-layer thickness in the fixed PCMO-layer thickness-based multilayers, clearly shows an antiferromagnetic-to-ferromagnetic transition, which is confirmed by the field-dependent magnetization described hereafter (see Fig. 3). Surprisingly, for the FM samples (i.e., with $n\geqslant 10$), the Curie temperature of the superlattices does not change significantly (226 K and 229 K for $n=12$ and $n=20$, respectively) with the LCMO-layer thickness.

The enhancement of FM is also observed in the field-dependent magnetization $M(H)$ of the superlattices with the increase in magnetic moments as the LCMO thickness increases. This is illustrated in the zero-field-cooled (ZFC) $M(H)$ at 10 K, recorded with a magnetic field oriented along the [100] and [001] directions of the substrate, for various samples ($n=4$, 8, 12, and 20), shown in Fig. 3. When looking in detail at the graph, we observe that the superlattice with

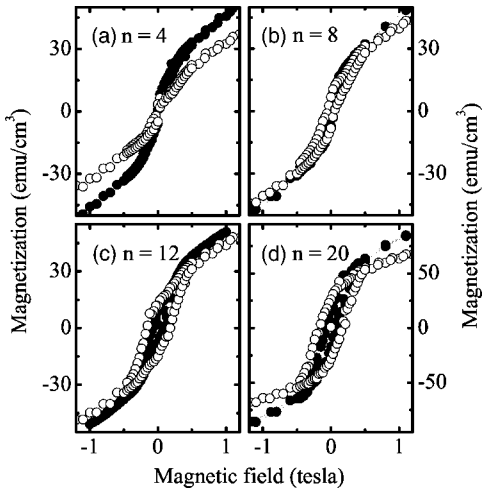

FIG. 3. Zero-field-cooled magnetic-field-dependent magnetization along in-plane (filled circle) and out-of-plane (open circle) directions of the superlattices with $n=4$, 8, 12, and 20 at 10 K.

the 4-u.c.-thick LCMO layer shows an ≈ 0.02 T coercive field (H_C) for both orientations of the magnetic field [Fig. 3(a)]. It also shows a small anisotropy, while the magnetization increases gradually with an increase in either the in-plane or out-of-plane magnetic field. A qualitatively similar hysteresis loop [Figs. 3(b)–3(d)], but with a higher value of the coercive field, is observed for the sample with a higher thickness of the LCMO layer ($n=8$, 12, and 20). Moreover, for the samples with $n>6$, the in-plane coercive field is smaller than the out-of-plane coercive field. This difference is clearly seen in Fig. 4(a), where the in-plane and out-of-plane coercive fields for various samples are plotted. The H_C increases with the increase in the LCMO-spacer-layer thickness and saturates for the sample with $n>10$. From this figure, it is observed that anisotropy in H_C appears for the sample with $n>6$. This anisotropy increases up to $n\approx 12$ and remains the same for higher values of n, although a relatively small increase in H_C has been observed in the superlattices with $n\leqslant 6$, compared to its constituents (LCMO and PCMO). Nevertheless, the exchange coupling at the interfaces is strongly enhanced H_C for superlattices with $n>6$. Since the magnetic interactions between the Mn ions in the bulk PCMO or LCMO do not lead to the enhancement of H_C, the origin of the enhancement must be from the exchange interaction between PCMO and LCMO at the interfaces. The fact that such features are strongly dependent on the stacking of the superlattices and viewing some recent results[21,22] reinforce this statement.

For the ideal antiferromagnetic state of the constituents, the magnetization of PCMO/LCMO should be independent of the magnetic field. The gradual increase in magnetization for both orientations of the magnetic field in the hysteresis loop (Fig. 3), indicates that the AFM sublattices contribute to the coupling energy at the interfaces when the difference in the orientation of its two magnetization sublattices deviates from 180°. The origin of the reorientation of the spins of the AFM sublattices could be due to the 3D coordinations of different *A*-site ions and/or the inhomogeneous magnetic phases. This will induce an extra interfacial anisotropy and

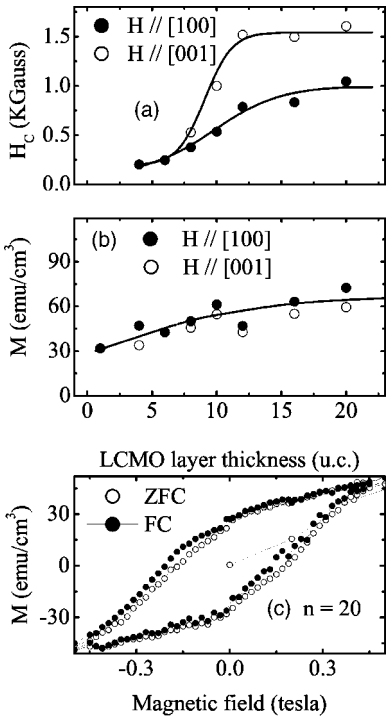

FIG. 4. (a) In-plane and out-of-plane coercive field at 10 K of the superlattices with different LCMO-layer thicknesses. (b) ZFC magnetization of various samples with different LCMO-layer thicknesses at 10 K at a 1 T magnetic field. The solid lines are guides to the eyes. (c) The zero-field-cooled and field-cooled (2 T) magnetic-field-dependent magnetization along the out-of-plane directions of the superlattices with $n=20$ at 10 K.

hence the anisotropy in the coercivity. The fluctuations of the AFM spin at the interfaces enhance the coercive field with the increase in the LCMO-layer thickness.[21] This effect is also realized in the net magnetizations of the superlattices. The net magnetizations of the superlattices at 1-T magnetic field with two orientations, at 10 K, for samples with various LCMO-layer thicknesses are shown in Fig. 4(b). As the LCMO-layer thickness increases from 1 u.c. to 10 u.c., the magnetization in $M(H)$, recorded at 10 K, under 1-T magnetic field increases 2 times, and for higher values of LCMO-layer thicknesses the magnetization increases to a negligibly small value. To explain these observations we consider the coherency and intrinsic inhomogeneities of the constituents. The presence of two different ionic-size elements at the *A* site in PCMO and LCMO leads to intrinsic inhomogeneities.[23] However, it is important at the interfaces due to the presence of La, Pr, and Ca. This introduction of an inherent or quenched disorder in the system results in a low-temperature regime that consists of ferromagnetically or antiferromagnetically ordered phases (inhomogeneous magnetic phases)[24] with randomly oriented order parameters. The presence of inhomogeneous magnetic phases in the bulk leads to three possible local magnetic coordinations (AFM-AFM, AFM-FM, and FM-FM) at the interfaces. The increase in the LCMO-layer thickness, i.e., the relaxation of strain, varies the strength of the exchange coupling at the PCMO/LCMO interfaces. As the LCMO-layer thickness increases from 1 u.c. to 9 u.c., the increase in magnetization is due to

the spin reorientation of the AFM sublattice at the interfaces. However, the relaxation of strain also induces its bulk-like properties in the LCMO layer. For ideal antiferromagnetic LCMO the magnetization of the sample with $n \geqslant 10$ should saturate. But the nonsignificant increase in magnetization for a sample with $n \geqslant 10$ could be due to the presence of inhomogeneous magnetic phases with the increase in microscopic to mesoscopic FM order parameters in LCMO.

We performed more measurements to confirm the AFM spin fluctuations at the PCMO/LCMO interface. In fact, the magnetic interactions across the interfaces between a ferromagnetic-spin system and an antiferromagnetic-spin system are generally known as exchange coupling, with phenomenological features such as enhancement of the coercive field H_C and a shifted hysteresis loop in the direction of the magnetic field.[4,5] It is usually observed on cooling the FM/AFM system below the Curie temperature of the FM through the Neel temperature T_N of the AFM in the presence of the magnetic field. We have used this formalism to verify whether the fluctuations of the AFM spin at the interfaces leads to the inhomogeneous magnetic phases in this system. The ZFC and FC hysteresis loops of the sample with $n=20$ at 10 K are shown in the Fig. 4(c). Though the constituent materials are antiferromagnetic, as the sample is cooled below room temperature in presence of a 2-T magnetic field, the origin of the hysteresis loop is shifted towards the negative-field axis. This confirms the presence of magnetic inhomogeneity in the samples.

We then tried to correlate these measurements with the transport as well as the structure of the samples. Thus, we also analyzed the structure and transport properties of these samples as a function of the LCMO-layer thickness. In oxide thin films, it is well known that the structural and transport properties are strongly dependent on the strains imposed by the substrate. This is particularly true for PCMO and LCMO thin films, as previously observed in similar films.[25,26] The lattice parameter of bulk PCMO ($a_{\mathrm{PCMO}}=3.802$ Å) and LCMO ($a_{\mathrm{LCMO}}=3.83$ Å) is larger than a_{LAO} with a lattice mismatch of +0.3% and +1.05%. Indeed, the epitaxial growth of PCMO on LAO provides in-plane compressive stress on PCMO. A similar kind of stress is also expected at the interfaces for the epitaxial growth of LCMO on PCMO, and such a difference might affect the physical properties. In the superlattices, the out-of-plane lattice parameter c increases with the increase in spacer-layer thickness and saturates for the sample with $n>10$ [Fig. 5(a)]. The c-axis lattice parameter of the superlattice with $n=1$ increases to $\approx 0.3\%$ as n increases to 20. This change is equal to the lattice mismatch between LAO and PCMO. Thus, we conclude that substrate-induced stress plays an important role in the structure of the superlattices, similarly to that in any manganite films.[26] However, relaxation does not change the qualitative behavior of temperature-dependent resistivity, but increases the conducting path. This leads to a lowering of the resistivity of the sample with an increase in the LCMO-layer thickness. As the sample is cooled below room temperature down to 100 K, it gains 3 orders of resistivity. This significant change in resistivity with temperature does not show remarkable variation in the LCMO-thickness dependence-resistivity curve at different temperatures [100 K and 300 K in Fig. 5(b)]. As the resistivity of all samples with various LCMO-layer thicknesses is very high below 100 K, it is prohibitive to compare the LCMO-thickness dependence resistivity below 100 K. Thus we present the change in the magnetoresistance ($\mathrm{MR}=[\rho(0)-\rho(H)]/\rho(H)$ at 100 K [Fig. 5(c)] as a function of the LCMO thickness. This notation for the MR is used for better resolution at the higher-LCMO-layer thickness. The crossover region from a strained to a strain-relaxed state with a LCMO-layer thickness appearing in the same region (close to $n=8$) as those observed in the variation of the coercive field [Fig. 4(a), at 10 K), magnetization [Fig. 4(b), at 10 K], resistivity, and magnetoresistance with the LCMO-layer thickness, indicate that the charge-spin coupling is correlated with the structure. This also suggests that both the crystallographic and/or magnetic reconstructions and relaxations are responsible for the physical properties of this system.

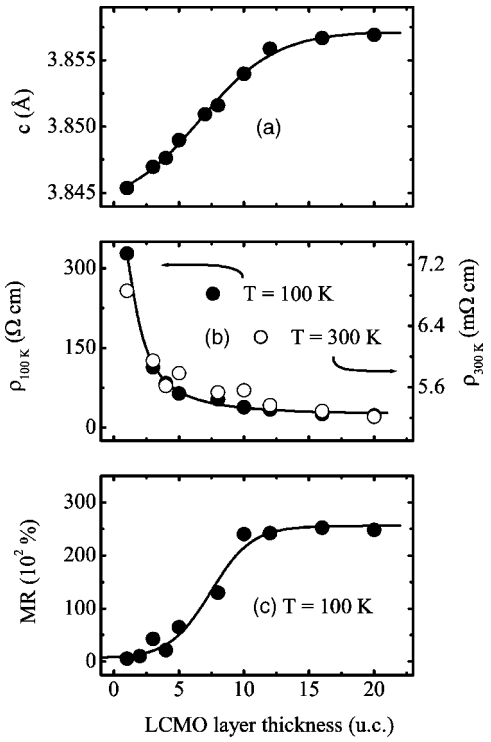

FIG. 5. (a), (b), and (c) Evolution of the out-of-plane lattice parameter, with resistivity at 100 K and magnetoresistance at 100 K under a 7 T applied magnetic field, respectively, of the superlattices for different LCMO-layer thicknesses. The solid lines are guides to the eyes.

In conclusion, the superlattices composed of $Pr_{0.5}Ca_{0.5}MnO_3$ and $La_{0.5}Ca_{0.5}MnO_3$ compounds were grown on (100) $LaAlO_3$ using pulsed laser ablation. The fixed PCMO-layer based PCMO/LCMO superlattices show an antiferromagnetic-to-ferromagnetic transition with an increase in the LCMO-layer thickness. For the coercive field, with magnetization at 1 T, c-axis lattice parameter, resistivity, and magnetoresistance show a crossover to their saturation values for the same LCMO-layer thickness. We attribute these correlations to the crystallographic and/or magnetic reconstructions and relaxations at the PCMO/LCMO interfaces. The coercive field is anisotropic to the orientations of

the magnetic field due to the magnetic inhomogeneity along the out-of-plane direction of the substrate. An enhancement of coercivity is observed in the superlattices with $n>6$. We have interpreted this enhancement as the AFM spin fluctuations at the interfaces. The presence of magnetic inhomogeneity is also confirmed from the ZFC and FC hysteresis loop of the superlattices. The transport behavior of the superlattices is similar to that of its constituents (i.e., insulating) but the increase in the LCMO-layer thickness induced a lower resistive conduction path. This study confirms the importance of the interfaces in superlattices that can be used to control physical properties in oxide materials.

We acknowledge financial support of Centre Franco-Indien pour la Promotion de la Recherche Avancee/Indo-French Centre for the Promotion of Advance Research (CEFIPRA/IFCPAR) under Project No. N2808-1.

*Email address: prellier@ensicaen.fr

[1] A. Orozco, S. B. Ogale, Y. H. Li, P. Fournier, Eric Li, H. Asano, V. Smolyaninova, R. L. Greene, R. P. Sharma, R. Ramesh, and T. Venkatesan, Phys. Rev. Lett. **83**, 1680 (1999).

[2] K. R. Nikolaev, A. Y. Dobin, I. N. Krivorotov, W. K. Cooley, A. Bhattacharya, A. L. Kobrinskii, L. I. Glazman, R. M. Wentzovitch, E. D. Dahlberg, and A. M. Goldman, Phys. Rev. Lett. **85**, 3728 (2000).

[3] P. Padhan, R. C. Budhani, and R. P. S. M. Lobo, Europhys. Lett. **63**, 771 (2003).

[4] J. Nogués and I. K. Schuller, J. Magn. Magn. Mater. **192**, 203 (1999).

[5] I. Panagiotopoulos, C. Christides, M. Pissas, and D. Niarchos, Phys. Rev. B **60**, 485 (1999).

[6] S. Dubourg, J. F. Bobo, J. C. Ousset, B. Warot, and E. Snoeck, J. Appl. Phys. **91**, 7757 (2002).

[7] M. Izumi, Y. Murakami, Y. Konishi, T. Manako, M. Kawasaki, and Y. Tokura, Phys. Rev. B **60**, 1211 (1999).

[8] P. Padhan and R. C. Budhani, Phys. Rev. B **67**, 024414 (2003).

[9] E. Fulcomer and S. H. Charap, J. Appl. Phys. **43**, 4190 (1972).

[10] K. Nishioka, C. Hou, H. Fujiwara, and R. D. Metzger, J. Appl. Phys. **80**, 4528 (1996).

[11] Z. Li and S. Zhang, Phys. Rev. B **61**, R14897 (2000).

[12] M. D. Stiles and R. D. McMichael, Phys. Rev. B **63**, 064405 (2001).

[13] K. Ueda, H. Tabata, and T. Kawai, Science **280**, 1064 (1998).

[14] K. S. Takahashi, M. Kawasaki, and Y. Tokura, Appl. Phys. Lett. **79**, 1324 (2001).

[15] Z. Jirak, S. Krupicka, Z. Simsa, M. Doulka, and S. Vratislma, J. Magn. Magn. Mater. **53**, 153 (1985).

[16] P. Levy, F. Parisi, G. Polla, D. Vega, G. Leyva, H. Lanza, R. S. Freitas, and L. Ghivelder, Phys. Rev. B **62**, 6437 (2000).

[17] C. N. R. Rao, Anthony Arulraj, A. K. Cheetham, and B. Raveau, J. Phys.: Condens. Matter **12**, R83 (2000).

[18] P. Padhan, W. Prellier, and B. Mercey, Phys. Rev. B **70**, 184419 (2004).

[19] W. Prellier, A. M. Haghiri-Gosnet, B. Mercey, Ph. Lecoeur, M. Hervieu, Ch. Simon, and B. Raveau, Appl. Phys. Lett. **77**, 1023 (2000).

[20] B. D. Cullity, *Elements of X-Ray Diffraction* (Addison-Wesley, London, 1978), p. 102.

[21] C. Leighton, J. Nogués, B. J. Jösson-Åkerman, and I. K. Schuller, Phys. Rev. Lett. **84**, 3466 (2000).

[22] C. Leighton, H. Suhl, Michael J. Pechan, R. Compton, J. Nogues, and I. K. Schuller, J. Appl. Phys. **92**, 1483 (2002).

[23] J. Burgy, M. Mayr, V. Martin-Mayor, A. Moreo, and E. Dagotto, Phys. Rev. Lett. **87**, 277202 (2001).

[24] J. W. Lynn, R. W. Erwin, J. A. Borchers, Q. Huang, A. Santoro, J.-L. Peng, and Z. Y. Li, Phys. Rev. Lett. **76**, 4046 (1996); J. M. De Teresa, M. R. Ibarra, P. A. Algarabel, C. Ritter, C. Marquina, J. Blasco, J. Garca, A. del Moral, and Z. Arnold, Nature (London) **386**, 256 (1997); M. Uehara, S. Mori, C. H. Chen, and S.-W. Cheong, Nature (London) **399**, 560 (1999); M. Fäth, S. Freisem, A. A. Menovsky, Y. Tomioka, J. Aarts, and J. A. Mydosh, Science **285**, 1540 (1999).

[25] P. Padhan, W. Prellier, Ch. Simon, and R. C. Budhani, Phys. Rev. B **70**, 134403 (2004).

[26] W. Prellier, Ph. Lecoeur, and B. Mercey, J. Phys.: Condens. Matter **13**, R915 (2001).